International Journal of Chemical Science
Online ISSN: 2523-2843, Print ISSN: 2523-6075; Impact Factor: RJIF 5.22
Received: 10-09-2019; Accepted: 13-10-2019
www.chemicaljournals.com
Volume 3; Issue 6; November 2019; Page No. 37-41

Synthesis and characterization of copper (ii) complex: Dna binding, nuclease and superoxide dismutase activity

Vikesh Kumar Singh[1], Anandveer Sindhu[2*]
[1, 2] Department of Chemistry, Meerut College Meerut, C.C.S. University Meerut, Uttar Pradesh, India

Abstract
A tridentate ligand L1 (*N*,1-di(pyridin-2-yl)methylamine) was converted into complex 2, copper complex of two picolinate anion. Ligand L1 was reacted with $CuCl_2 \cdot 2H_2O$ in presence of triethylamine and a facile oxidation of azomethine function to carboxylic acid was observed. The resultant complex 2 afforded superoxide dismutase (SOD) activity and IC_{50} value was found to be 2.60 μM in xanthine/xanthine oxidase nitroblue tetrazolium assay. This small molecule SOD mimic exhibited nuclease activity by cleaving pBR322 DNA oxidatively in presence of 2-mercaptoethanol.

Keywords: copper, DNA binding, nuclease, SOD activity

Introduction
Studies on copper-assisted transformation of organic functional groups are fundamentally important because of their applications in copper catalyzed synthesis of novel metal complexes and organic molecules [1, 4]. As a part of our ongoing research, we were interested in synthesizing novel copper complexes which exhibit superoxide scavenging activity (SOD activity) as well as nuclease activity because such type of complexes are important in metallopharmaceutical research [5]. In the present work we report an unprecedent oxidation of azomethine function of L1 and facile synthesis of a complex 2 [6, 7] by the reaction of ligand L1 in presence of copper chloride salt and triethylamine in methanol (Scheme 1). Here, we proposed that in first step of reaction the the Cu^{2+} ion form an intermediate complex 1 with ligand L1. There has been considerable current interest for the synthesis of metal-organic frameworks (MOFs) because of their applications in magnetism, photochemistry and catalytic activity [8]. The complex 2 possesses one dimensional chain structure (vide infra), is an important precursor for the synthesis of metal-organic frameworks [6, 7] There are several reports [6, 8] where 2 was used as a building block for metallo-supramolecular assemblies however, SOD activity and DNA interaction studies of this metalloligand remained unknown.

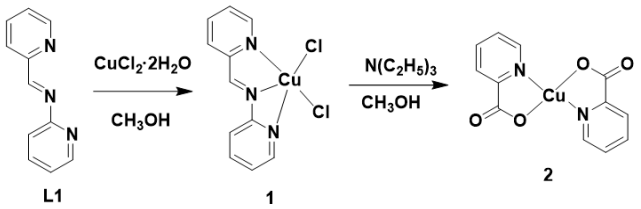

Scheme 1: Conversion of ligand L1 into intermediate copper complex 1 and complex 2.

Copper is an important metal for the synthesis of artificial nucleases because this biologically relevant metal ion has high affinity for nucleobases and copper complexes possess biologically accessible redox properties [9]. It has been documented in the literature that multinuclear copper Complexes were found to be more efficient and selective in DNA interactions [9, 13]. In this work, we have performed the interaction of DNA with complex 2, nuclease activity and SOD activity.

Experimental Section
Materials and measurements
2–mercaptoethanol, hydrogenperoxide and L-histidine (S. D. Fine, Mumbai, India), sodium azide, triethylamine (Sigma Aldrich, Steinheim, Germany), ethylenediamine tetraacetic acid and copper perchlorate hexahydrate (Merck Limited, Mumbai, India), were used as obtained. The supercoiled pBR322 DNA and CT DNA were purchased from Bangalore Genei (India) and stored at 4 °C. Agarose (molecular biology grade) and ethidium bromide were obtained from Sigma Aldrich. Tris (hydroxy methyl) amino methane–HCl (Tris–HCl) buffer was prepared in deionised water. Solvent used for spectroscopic studies were HPLC grade and purified by standard procedure before use.
Elemental analysis of complex was carried out on Elemental model Vario EL–III. Infrared spectra were recorded as KBr pellets on a Nicolet NEXUS Aligent 1100 FT–IR Spectrometer, using 50 scans and were reported in cm^{-1}. Electronic spectra were recorded in methanol, DMF and phosphate buffer solution with Evolution 600, Thermo scientific, UV–vis spectrophotometer using cuvettes of 1 cm path length. Fluorescence spectra were recorded by Varian Cary (Eclipse) fluorescence spectrophotometer.

Synthesis of complex 2
A 2 mL solution of $CuCl_2 \cdot 2H_2O$ (0.180g, 0.5 mmol) was added to a 5 ml methanolic solution of L1 (0.137g 0.5 mol) in a round bottom flask. An immediate color change from yellow to green was observed after the addition of copper salt. Addition of triethylamine (~ 100 mg) to the above reaction mixture afforded immediate color change from green to blue. After three days needle–shaped, sky blue crystals were deposited and collected by filtration. (Yield: 48%). Anal. Calcd for C_{12} H_{12} N_2O_6Cu (343.78): C, 41.92;

H, 3.52; N, 8.15. Found C, 41.95; H, 3.58; N, 8.19. FTIR (KBr disks, cm^{-1}): 3430 (br), 1643 (s), 1604 (s), 1347 (s), 1285(m), 1048 (m), 777 (m). UV–vis (phosphate buffer; $\lambda_{max,}$ nm (ε, ($M^{-1}cm^{-1}$)): 264 (10400).

DNA binding and cleavage experiments

All DNA binding experiments were carried out in 0.1 M phosphate buffer (pH 7.2) using a solution of calf thymus (CT) DNA which gave a ratio of UV–vis absorbance at 260 and 280 nm (A_{260}/A_{280}) of *ca.* 1.8, indicating that the CT–DNA was sufficiently protein free. The concentration of DNA solution was determined by UV absorbance at 260 nm and the extinction coefficient ε_{260} was taken 6600 cm^{-1} as reported in the literature [14].

Fluorescence quenching experiments were carried out by the successive addition of **2** to the DNA (25 µM) solutions containing 5 µM ethidium bromide (EB) in 0.1 M phosphate buffer (pH 7.2). These samples were excited at 250 nm and emissions were observed between 500 and 700 nm. Stern–Volmer quenching constants were calculated using the given equation

$I_0/I = 1 + K_{sv}Q$

Where I_0 and I are the fluorescence intensities in the absence and presence of complex and Q is the concentration of quencher (complexes). K_{sv} is a linear Stern–Volmer constant and given by the ratio of slope to intercept in the plot of I_0/I versus Q [14].

Cleavage of plasmid DNA was monitored by using agarose gel electrophoresis. Supercoiled pBR32 DNA (40 ng) in (TBE) Tris–boric acid–EDTA buffer (pH 8.2) was treated with 2 (100 µM) in the presence or absence of additives. The reductive DNA cleavage by the complex was studies in the presence of H_2O_2 (200 µM, oxidizing agent) or 2–mercaptoethanol (200 µM, reducing agent) and DMSO, ethanol, urea, NaN_3, D_2O, L-histidine, NaCl (20 mM, ROS scavenger) and catalase (10U). The samples were incubated for 1.5 h at 37 °C, added loading buffer (25% bromophenol blue and 30% glycerol). The agarose gel (0.8%) containing 2 µL (10 mg/mL stock) of ethidium bromide (EB) was prepared and the electrophoresis of the DNA cleavage products was performed on it. The gel was run at 60 V for 2 h in TBE buffer and the bands were identified by placing the stained gel under an illuminated UV lamp. The fragments were photographed by using gel documentation system (BIO RAD).

Superoxide dismutase activity

SOD activity of the complex **2** was determined by using the ability to inhibit the reduction of nitroblue tetrazolium (NBT) by superoxide radical $O_2^{\cdot -}$ generated by the xanthine/xanthine oxidase method [5, 16, 17]. The reaction system contained 0.2 mM xanthine, 0.6 mM NBT and 50 mU/mL xanthine oxidase to start the reaction in 0.1 M phosphate buffer at pH 7.8. The extent of NBT reduction was followed spectrophotometrically by measuring the absorbance at 555 nm. Each experiment was performed in duplicate and the SOD activity has been defined as the concentration of the tested compound for the 50% inhibition of the NBT reduction (IC_{50} value) by superoxide produced.

X–ray Crystallography

The X–ray data collection and processing for 2 performed on Bruker Kappa Apex–II CCD diffractometer by using graphite monochromated Mo–Kα radiation (λ = 0.71070 Å) at 296 K. Crystal structures were solved by direct methods. Structure solution, refinement and data output were carried out with the SHELXTL program [15]. All non–hydrogen atoms were refined anisotropically. Hydrogen atoms were placed in geometrically calculated positions and refined using a riding model. Images were created with the Diamond program [16].

Table 1: Crystal data and structure refinement for $[Cu(pic)_2]\cdot 2H_2O$.

Empirical formula	C12 H12 Cu N2 O6
Formula weight	343.78
Temperature	123(2) K
Wavelength	0.71073 Å
Crystal system	Triclinic
Space group	P -1
a	5.0861(10) Å
b	7.5143(15) Å
c	9.0690(18) Å
α	75.98(3)°
β	85.14(3)°
γ	72.19(3)°
Volume	320.14(11) Å3
Z	1
Density (calculated)	1.783 Mg/m3
Absorption coefficient	1.737 mm-1
F(000)	175
Crystal size	0.37 x 0.24 x 0.16 mm3
Goodness-of-fit on F2	1.154
Final R indices [I>2sigma(I)]	R1 = 0.0257, wR2 = 0.0705

Results and Discussion

Synthesis and Characterization

The intermediate complex 1 was generated in situ by the reaction of L1 and $CuCl_2\cdot 2H_2O$. Addition of triethylamine to the reaction mixture afforded generation of blue colored complex 2. Blue crystalline compound was isolated via slow evaporation of the above reaction mixture within 3−4 days.

The resultant complex 2 was characterized by FTIR (Figure 1) and UV-visible spectra (Figure 2). Molecular structure determination of complex 2 by X-ray crystallography revealed that the resultant complex was $[Cu\ (pic)_2]\cdot 2H_2O$. All the parameters and selected bond lengths and bond angles for $[Cu(pic)_2]$ are shown in Table 1. A perspective view of packing diagram of 2 is shown in Figure 3. The structure and the spectroscopic properties were similar to the data reported in the literature [20, 24].

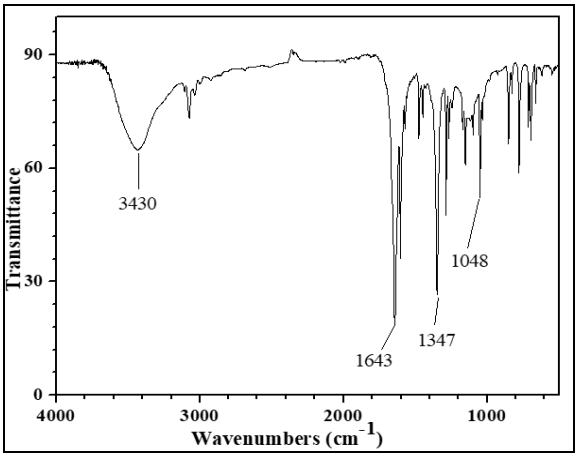

Fig 1: FT-IR spectrum of complex **2**.

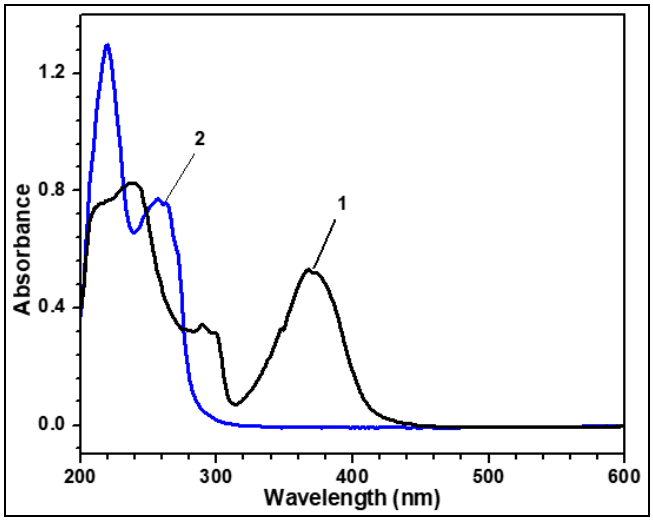

Fig 2: UV-visible spectra of conversion of complex **1** (50 µM) into **2** by triethylamine.

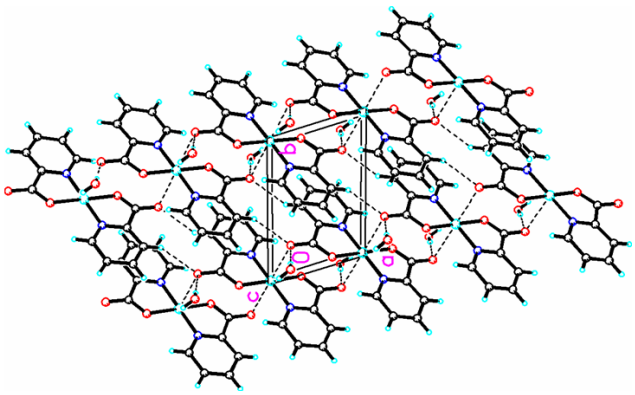

Fig 3: Packing diagram of complex 2 with unit cell (showing 50% thermal probability ellipsoids)

Investigation of literature revealed that apart from the direct reaction between picolinic acid and copper salt, [17] there were always a tendency of copper complexes derived from 2-substituted pyridine ligands to form complex 2 [18, 21]. However to the best of our knowledge there was no report on oxidation of copper coordinated azomethine function for the synthesis of 2. Oxidation of copper coordinated azomethine function into aldehyde function [2] and amide group [3, 4, 22] was known in the literature. A facile hydrolysis of azomethine function in copper complexes was reported by Dash and coworkers in presence of acid and base [23, 24]. However in the reaction described above oxidation of azomethine function was observed and azomethine function was converted to carboxylic acid group. We want to mention here that in presence of excess of triethylamine a mixture of copper salt and pyridine 2-aldehyde (1:1 equivalent) did not afford complex 2. Further investigation of the mechanism is under progress.

Redox properties

The redox behavior of complex **2** was investigated by cyclic voltammetry at a glassy carbon electrode using Ag/AgCl reference electrode with internal standard ferrocene in DMF solution at 298 K (Figure 4). The curve clearly indicated a quasireversible Cu(II)/Cu(I) couple having $E_{1/2}$ value –0.482 V vs Ag/AgCl electrode and ΔE value of 0.125 V.

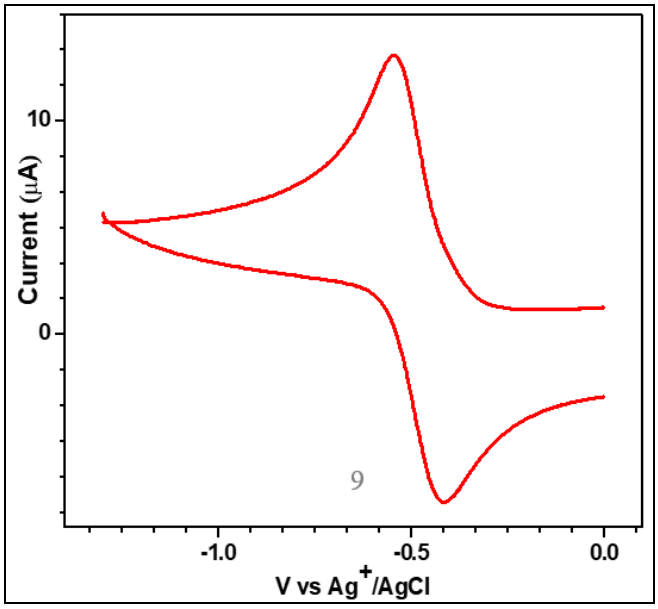

Fig 4: Cyclic voltammograms of a 10^{-3} M solution of complex **2** in DMF in presence of 10^{-3} M solution of ferrocene and 0.1 M TBAP as a supporting electrolyte, glassy–carbon as a working electrode and Ag/AgCl as reference electrode; scan rate 0.1 V/s.

Superoxide dismutase activity

SOD activity was monitored by reduction of nitro blue tetrazolium (NBT) with $O_2^{\cdot -}$ generated by xanthine/xanthine oxidase system [25]. As the reaction proceeds, the farmazan color is developed and a color change from yellow to blue appeared which was associated with an increase in the absorbance at 555 nm. The rate of absorption change was determined and the concentration required to produce 50% inhibition (IC_{50}) be obtained by graphing the rate of NBT reduction vs complex concentration. Complex **2** showed IC_{50} values of 2.60 µM (Figure 5) which was better than the reported value for $CuSO_4$ however much lower than the native enzyme CuZnSOD. The potency of **2** was higher than the similar bis complexes of copper with nicotinic acid, phthalic acid, salicylic acid and anthranilic acid [26].

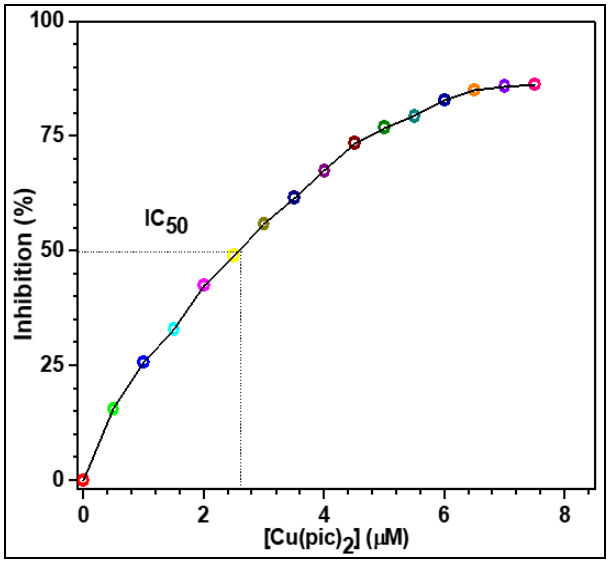

Fig 5: Dependence of the inhibition of NBT reduction by superoxide on the concentration of 2. Incubation time was 5 min.

DNA binding and nuclease activity

In order to understand the mode of DNA-binding for complex **2**, electronic absorption spectral and fluorescence quenching studies were investigated. We were unable to determine K_b value because the complex and DNA both had peak(s) near 260 nm and the complex was devoid of any other peak in the absorption spectrum (Figure 6). Ethidium bromide fluorescence quenching studies were examined (Figure 7) and Stern –Volmer constant (K_{sv}) was calculated by plot of I_0/I vs complex **2**. The constant K_{sv} was found to be 1.24 x 10^4 which was less than the values reported for intercalators [27]. The above data indicated that the complex showed probable surface interaction with DNA via external binding.

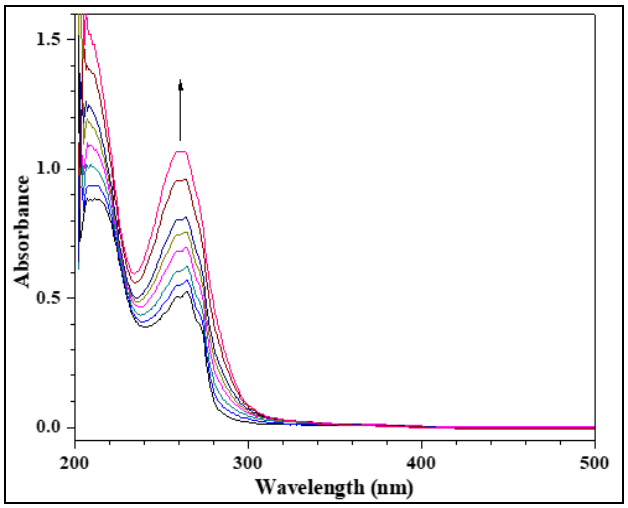

Fig 6: Absorption spectra of complex 2 (50 µM) in 0.1 M phosphate buffer (pH 7.2) in the presence of increasing amounts of [DNA] = 0 – 71.62 µM.

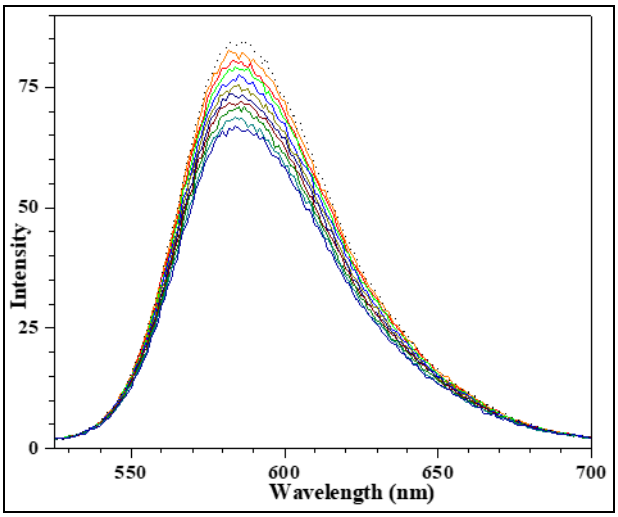

Fig 7: Fluorescence emission spectra of the EB–DNA in 0.1 M phosphate buffer (pH 7.2) in the absence (dashed line) and presence (solid line) of complex. [EB] = 10 µM, [DNA] = 25 µM, [2] = 0 – 20 µM, λ_{ex} = 250 nm and λ_{em} = 602 nm.

We extended our DNA interaction studies by examining the nuclease activity of the complex 2. The cleavage of supercoiled pBR322 DNA by the complex and concomitant formation of nicked (NC) and linear (LC) DNA were studied by gel electrophoresis in Tris–boric acid–EDTA buffer (TBE).

DNA cleavages were performed aerobically in the presence of H_2O_2 and 2–mercaptoethanol and following are the major findings. First, in the control experiment the complex 2 itself did not show (may be negligible) nuclease activity till concentration of 100 µM (lane 5, Figure 8). Second, the complex did not exhibit DNA cleavage activity in presence of H_2O_2 even at high concentration (600 µM) (lane 6-8, Figure 8) whereas complex exhibited nuclease activity in presence of BME (lane 9-14, Figure 8). Interestingly, the DNA got converted to NC as well as LC form in the presence 2–mercaptoethanol (200 µM) as we increased the concentration of complex from 25 to 200 µM.

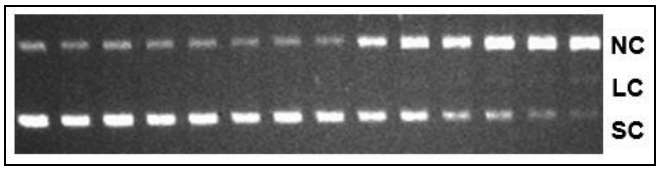

Fig 8: Gel electrophoresis separations showing the cleavage of supercoiled pBR322 DNA (40 ng) by 2 in presence of H_2O_2 and BME. Incubated at 37 °C for 1.5 h. Key: lane 1, DNA control; lane 2, DNA + H_2O_2 (200 µM); lane 3, DNA + BME (200 µM); lane 4, DNA + $Cu(ClO_4)_2 \cdot 6H_2O$ (100 µM); lane 5, DNA + 2 (100 µM); lane 6, DNA + 2 (100 µM) + H_2O_2 (200 µM); lane 7, DNA + 2 (100 µM) + H_2O_2 (400 µM); lane 8, DNA + 2 (100 µM) + H_2O_2 (600 µM); lane 9-14, DNA + BME (200 µM) + 2 = 25, 50, 75, 100, 150, 200 µM respectively; SC = supercoiled form, NC = nicked circular form, LC = linear form.

The time dependence of the cleavage reactions was examined for 2 (100 µM) in presence of BME (200 µM). The reactions were monitored over a period of 10– 120 min at 37 °C and the incubation time increased the conversion of SC form to NC and LC form (lane 7-11, Figure 9). For complete conversion of SC form to NC and LC form, 90 min incubation was enough (Figure 9). The concentration of 2-mercaptoethanol (50-200 µM) also enhance the nuclease activity at constant concentration of 2 (100 µM).

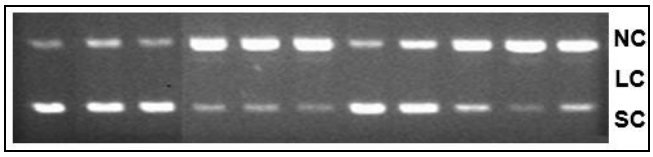

Fig 9: Gel electrophoresis separations showing the cleavage of supercoiled pBR322 DNA (40 ng) by complex 2 (100 µM) in presence BME. Incubated at 37 °C for 1.5 h. Key: lane 1, DNA control; lane 2, DNA + BME (600 µM); lane 3, DNA + 2; lane 4, DNA + 2 + BME (200 µM); lane 5, DNA + 2 + BME (400 µM); lane 6, DNA + 2 + BME (600 µM); lane 7-11, DNA + 2 + BME (200 µM) + 10, 30, 60, 90, 120 min incubation respectively. SC = supercoiled form, NC = nicked circular form, LC = linear form.

The presence of diffusible radical species can be diagnosed by monitoring the quenching of DNA cleavage in the presence of radical scavengers in solution [9, 13]. Radical scavengers were added to the reaction of 2 with 2–mercaptoethanol. The individual addition of radical scavengers like DMSO, ethanol, urea, NaN_3, D_2O, L-histidine, NaCl (20 mM) and catalase (10 U). The addition of hydroxyl radical scavengers such as DMSO and ethanol inhibited the conversion of SC form to NC and LC form (lane 3-4, Figure 10) however, urea did not inhibit the conversion of SC form (lane 5, Figure 10). These results suggest that hydroxyl radicals may be the reactive species involved in the cleavage process [9]. Addition of singlet

oxygen scavengers NaN_3 and L-histidine inhibited the DNA cleavage activity (lane 6 and 8, Figure 10) which suggests that $^1O_2$ or any other singlet oxygen–like entity participate in the DNA strand scission [10, 13]. Nuclease activity was not affected by D_2O (which showed the life time enhancement of singlet oxygen) and NaCl. Probable participation of hydrogen peroxide was also excluded due to the results of addition of catalase during cleavage reaction (lane 9, Figure 10).

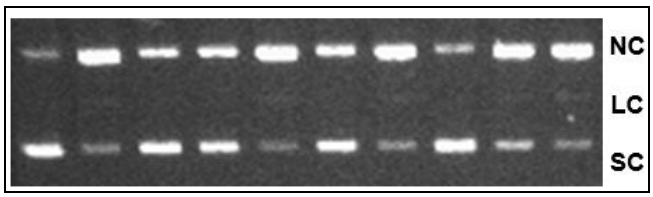

Fig 10: Gel electrophoresis separations showing the cleavage of supercoiled pBR322 DNA (40 ng) by 2 (100 µM) in presence of BME (200 µM). Incubated at 37 °C for 1.5 h. Key: lane 1, DNA; lane 2, DNA + 2 + BME; lane 3-10, DNA + 2 + BME + DMSO (20 mM), ethanol (20 mM), urea (20 µM), NaN_3 (20 mM), D_2O (20 mM), L-histidine (20 mM), catalase (10 U), NaCl (20 mM) respectively; SC = supercoiled form, NC = nicked circular form, LC = linear form.

On the basis of these results, we propose that the reactive oxygen species (ROS) which are participating in nuclease activity may be hydroxyl radical ($OH^•$) and/or singlet oxygen ($^1O_2$). On the basis of all these results, we propose that the compound showed weak interaction with DNA and the Cu(II) centre was reduced to Cu(I) species in presence of reducing agent. These subsequent react with dioxygen molecule to give the hydroxyl radicals and some singlet oxygen species which are responsible for DNA cleavage.

Conclusions

In conclusion, a facile synthesis of complex 2 via oxidation of azomethine function was described. This report is an unique example of copper assisted transformation of azomethine to carboxylic acid function. The complex showed SOD activity and afforded an IC_{50} value of 2.60 µM by xanthine/xanthine oxidase NBT assay. The complex interacted with DNA probably via surface and/or external binding and exhibited nuclease activity in presence of reducing agent only. Investigation of the mechanism predicted probable participation of reactive oxygen species (ROS) like hydroxyl radical ($OH^•$) and/or singlet oxygen ($^1O_2$) in nuclease activity.

Acknowledgments

Authors are thankful to Merrut College Meerut to provied infrastructure.

References

1. Sangeetha NR, Pal S, Pal S. Polyhedron, 2000; 19:2713.
2. Andrez JC. Tet Lett, 2009; 50:4225.
3. Padhi SK, Manivannan V. Inorg Chem, 2006; 45:7994.
4. Sahu R, Jena HS, Manivannan V. Inorg Chim Acta. 2010; 363:1448.
5. Zhang CX, Lippard SJ, Curr Opin Chem Biol. 2003; 7:481.
6. Biswas C, Mukherjee P, Drew MGB, Gomez-Garcia CJ, Clemente-Juan JM, Ghosh A. Inorg Chem, 2007; 46:10771.
7. Biswas C, Drew MCB, Escudero D, Frontera A, Ghosh A. Eur J Inorg Chem, 2009; 15:2238.
8. Jeon R, Ababei R, Lecren L, Li YG, Wernsdorfer W, Roubeau O, *et al*. Dalton Trans, 2010; 39:4744.
9. Chen J, Wang X, Shao Y, Zhu J, Zhu Y, Li Y, *et al*. Inorg Chem, 2007; 46:3306.
10. Humphreyes KJ, Johnson AE, Karlin KD, Rokita SE. J Biol Inorg Chem, 2002; 7:835.
11. Tu C, Shao Y, Gan N, Xu Q, Guo Z. Inorg Chem, 2004; 43:4761.
12. Humphreyes KJ, Karlin KD, Rokita SE. J Am Chem Soc, 2001; 123:5588.
13. Humphreyes KJ, Karlin KD, Rokita SE. J Am Chem Soc, 2002; 124:8055.
14. Muralisankar M, Bhuvanesh NSP, Sreekanth A. New J Chem, 2016; 40:2661.
15. Sheldrick GM. Acta Crystallogr Sect A, 1990; 46:467.
16. Klaus B. University of Bonn, Germany DIAMOND, Version 1.2 c, 1999.
17. Faure R, Loiseleur H, Thomas-David G. Acta Crystallogr Sect B, 1973; 29:1890.
18. Segl P, Jamnicky M, Koman M, Sima J, Glowiak T. Polyhedron, 1998; 17:4525.
19. Barandika MG, Serna ZE, Urtiaga MK, de Larramendi JIR, Arriortua MI, Cortes R, *et al*. Polyhedron, 1999; 18:1311.
20. Mikuriya M, Azuma H, Nukada R, Sayama Y, Tanaka K, Lim JW, *et al*. Bull Chem Soc Jpn, 2000; 73:2493.
21. Du M, Bu XH, Shionoya M, Shiro M. J Mol Struct, 2002; 607:155.
22. Brewer G, Kamaras P, Prykov S, Shang M, Scheildt WR. J Chem Soc Dalton Trans, 1999, 4511.
23. Dash AC, Dash B, Mahapatra PK, Patra MJ. Chem Soc Dalton Trans, 1983, 1503.
24. Dash AC, Dash B, Panda D. J Org Chem, 1985; 50:2905.
25. Goldstein S, Czapski G. Superoxide Dismutase, in: Punchard NA, Kelly FJ, (Eds.), 1996.
26. Free Radicals – A Practical approach, Oxford University Press, UK.
27. Suksrichavalit T, Prachayasittikul S, Piacham T, Isarankura C, Nantasenamat C, Prachayasittikul V, *et al*. Molecules, 2008; 13:3040.
28. Dong FY, Li YT, Wu ZY, Sun YM, Liu ZQ, Song YL, J Inorg Organomet Polym, 2008; 18:398.